White Rose Research Online

eprints@whiterose.ac.uk
https://eprints.whiterose.ac.uk
Universities of Leeds, Sheffield and York

Deposited via The University of Sheffield.

White Rose Research Online URL for this paper:
https://eprints.whiterose.ac.uk/id/eprint/238484/

Version: Accepted Version

Article:
Milanesi, L., Hunter, C.A., Tzokova, N. et al. (2011) Versatile low-molecular-weight hydrogelators: Achieving multiresponsiveness through a modular design. Chemistry – A European Journal, 17 (35). pp. 9753-9761. ISSN: 0947-6539

https://doi.org/10.1002/chem.201100640

This is the peer reviewed version of the following article: Milanesi, L., Hunter, C.A., Tzokova, N., Waltho, J.P. and Tomas, S. (2011), Versatile Low-Molecular-Weight Hydrogelators: Achieving Multiresponsiveness through a Modular Design. Chem. Eur. J., 17: 9753-9761, which has been published in final form at https://doi.org/10.1002/chem.201100640. This article may be used for non-commercial purposes in accordance with Wiley Terms and Conditions for Use of Self-Archived Versions. This article may not be enhanced, enriched or otherwise transformed into a derivative work, without express permission from Wiley or by statutory rights under applicable legislation. Copyright notices must not be removed, obscured or modified. The article must be linked to Wiley's version of record on Wiley Online Library and any embedding, framing or otherwise making available the article or pages thereof by third parties from platforms, services and websites other than Wiley Online Library must be prohibited.

Reuse
Items deposited in White Rose Research Online are protected by copyright, with all rights reserved unless indicated otherwise. They may be downloaded and/or printed for private study, or other acts as permitted by national copyright laws. The publisher or other rights holders may allow further reproduction and re-use of the full text version. This is indicated by the licence information on the White Rose Research Online record for the item.

Takedown
If you consider content in White Rose Research Online to be in breach of UK law, please notify us by emailing eprints@whiterose.ac.uk including the URL of the record and the reason for the withdrawal request.

UNIVERSITY OF LEEDS
University of Sheffield
UNIVERSITY of York

((will be filled in by the editorial staff))

Versatile low molecular weight hydrogelators: achieving multiresponsiveness via a modular design

Lilia Milanesi,*[a] Christopher Hunter, [b] Nadejda Tzokova,[b] Jonathan P. Waltho [c] and Salvador Tomas* [a]

Abstract: Multi responsive LMWH are ideal candidates for the development of smart soft nanotechnology materials. Its synthesis is however very challenging. On the one hand, *de novo* design is hampered by our limited ability to predict the assembly of small molecules in water. On the other hand, modification of pre-existing LMWH is limited by the number of different stimuli-sensitive chemical moieties that can be introduced into a small molecule without seriously disrupting the ability to gelate water. Here we report the synthesis and characterization of multi-stimuli LMWH, based on a modular design, composed of an hydrophobic di-sulfide aromatic moiety, a maleimide linker and an hydrophilic section based on an amino-acid, here *N*-acetyl-L-cysteine. As most LMWH, our gelators experience reversible gel-to-sol transition following temperature changes. Additionally, the *N*-acetyl-L-cysteine moiety allows reversible control of the assembly of the gel by pH changes. The reduction of the aromatic disulfide triggers a gel-to-sol transition that, depending on the design of the particular LMHG, can be reverted by re-oxidation of the resulting thiol. Finally, the hydrolysis of the cyclic imide moieties provides an additional trigger for the gel-to-sol transition with a timescale that is appropriate for its use in drug delivery applications. The efficient response to the multiple external stimuli, coupled to the modular design of the makes those LMWH an excellent starting point for the development smart nanomaterials with applications that include controlled drug release. These hydrogelators, which were discovered by serendipity rather than design, suggest nonetheless a general strategy for the introduction of multiple stimuli-sensitive chemical moieties: to offset the introduction of hydrophilic moieties with additional hydrophobic ones, in order to minimize the upsetting of the critical hydrophobic-hydrophilic balance of the LMWH.

Keywords: Gels • Self-assembly • Multiresponsiveness • disulfide • maleimide

Introduction

Low molecular weight gelators (LMWG) are small molecules that self-assemble into long fibers, resulting in the gelation of the solvent.[1-3] These fibers are held together by non-covalent, weak interactions between the individual LMWG molecules.[1,2,4-7] The gelating properties of LMWG can be modulated by modifying the strength of these interactions, as demonstrated by the thermal reversibility of the gel to sol transition.[1-3,7, 8-11] The close relationship between the structural integrity of the gel and the weak interactions allows tuning the macroscopic properties of LMWG more efficiently than polymeric (covalently-assembled) gels.[1,12-15] LMWG are therefore ideal candidates for the development of stimuli-responsive smart materials. [1,13, 16,17]

Low molecular weight hydrogelators (LMWH), i.e. LMWG that gelate water, are of special interest for the development of bio-compatible materials.[5,8,13,18,19] For example, LMWH with applications in regenerative medicine, tissue engineering, drug delivery, biosensing and catalysis have been reported.[12,13,20-28] For many LMWH the ability to gelate water can be modulated as a response to one particular external stimulus (other than a temperature change). In these LMWH responsiveness is commonly achieved by adding chemical moieties that are sensitive to the external stimulus of interest (e.g., to pH, light, ionic strength, enzymatic reactions or the addition of ligands) to a pre-existing gelating scaffold.[10,13,14,29-33] The changes in these chemical moieties brought about by the stimulus lead either to a gel to sol or a sol to gel transition that in some cases may be be reversibly controlled. Whilst many LMWH responsive to a single stimulus have been reported to date, examples of irreversible or

[a] Dr. L. Milanesi, Dr. S.Tomas,
Department of Biological Sciences, School of Science, Birkbeck University of London, London WC1E 7HX, UK
Fax: (+)44 (0)20 7631-6246
E-mail: l.milanesi@mail.cryst.bbk.ac.uk, s.tomas@bbk.ac.uk

[b] Prof. C. A. Hunter, Dr. N. Tzokova
Centre for Chemical Biology, Krebs Institute for Biomolecular Science, Department of Chemistry, The University of Sheffield, Sheffield S3 7HF, UK

[c] Prof. J. P. Waltho
Department of Molecular Biology and Biotechnology, The University of Sheffield, Sheffield S10 2TN, UK and Faculty of Life Sciences and Manchester Interdisciplinary Biocentre, The University of Manchester, Manchester M1 7DN, U.K

Supporting information for this article is available on the WWW under

reversible multi-responsive LMWH are still rare, in spite of the superiority of these materials relative to single-responsive gelators.[13,22,28,29,31,32] However achieving multi-responsiveness is a challenging task. LMWH are amphiphilic molecules whose ability to assemble into gel-forming fibres depends to a large extent on the hydrophobic-hydrophilic balance, finely tuned by the presence of intermolecular interactions such as H-bonds.[1-3,11] Changes in this balance brought about by the addition of several stimuli-responsive moieties may easily lead to loss of the ability of the molecule to assemble into a hydrogel.[11] The impact of these moieties may be reduced by offsetting the effect of an additional moiety that is hydrophilic in nature with the presence of another one that is hydrophobic, each of them located in appropriate parts of the molecule. Herein we report multi-stimuli responsive LMWHs based on this approach (Scheme 1). A hydrophobic disulfide bond, located in the hydrophobic part of the molecule provides reversible responsiveness to redox stimuli.[11,34,35] Hydrophilic carboxylic acid moieties, located in the hydrophilic part of the molecule, provide reversible responsiveness to changes in pH.[10,29,31,32] Additionally, the presence of hydrolysable cyclic imides provides a third mechanism for gel disassembly, albeit a non reversible one.

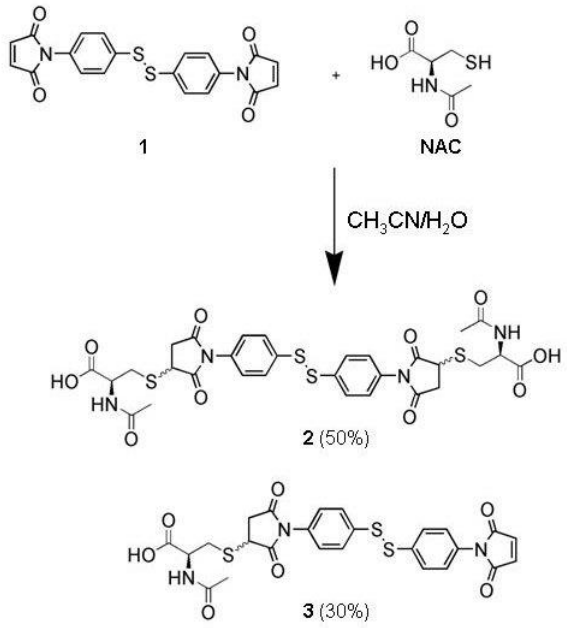

Scheme 1.

Results and Discussion

Synthesis and characterization of the hydrogelators. Compounds **2** and **3** were prepared in one pot reaction from the bismaleimide derivative 1 using a procedure previously reported for the synthesis of protein crosslinking reagents (Scheme 1).[36,37] Addition of N-acetyl-L-cysteine (NAC) over **1** yielded a mixture of **2** and **3** in a 5:3 ratio, that where separated by preparative RP-HPLC. The water gelating ability of **2** and **3** was readily observed when evaporating the corresponding aqueous fractions containing the gelators. Both **2** and **3** were obtained as a mixture of diastereoisomers due to the stereochemistry typical of this type of Michael addition reactions. The mixture of diastereoisomers is approximately 1:1 for both compounds as shown by NMR and no attempts were made to separate each diastereoisomers for the purpose of this work (See Supplementary Material and Figure 1S, 2S and 3S).

The imide groups of **2** and **3** are susceptible of base-catalyzed hydrolysis in aqueous solution, a reaction observed in many maleimide bioconjugates and malemide-thiols adducts in general.[38,39] The hydrolysis of each imide group yields two additional carboxylic acid groups that may affect the solubility of **2** and **3** and their ability to gelate water (Scheme 1S). We therefore studied the kinetic stability of **2** and **3** against hydrolysis by monitoring changes in the UV/Vis spectra of solutions (eg. below the critical gelation concentration, CGC) of both compounds. As expected the rate constants are pH dependent (Table 1 and Figure 4S). The hydrolysis of the succinimide moiety is relatively slow and similar for both **2** and **3** (t 1/2 = 12 h for 2 and 13 h for 3 at pH 7.2, see Table 1). The hydrolysis of the maleimide moiety of **3** is on the other hand nearly one order of magnitude faster relative to hydrolysis of the succinimide group consistent with the literature (t 1/2 imide moiety of 3 = 1.5 h, Table 1 and Figure 4S).[38,39] In the gel state the hydrolysis of the imide groups is markedly slower and it is important for the stability and potential application of the hydrogelators as explained in the following sections.

Table 1. Observed pseudo first order rate constants for hydrolysis of solutions of **2** and **3** and hydrogel **3**. For both compounds in solution (sol), k_{obs} is the rate constant for hydrolysis of the succinimide moiety whilst k'_{obs} is the rate constant for the hydrolysis of the maleimide moiety of **3**. For hydrogel **3** k'_{obs} is the rate constant of hydrolysis of both the imide moieties. Likewise t' ½ is the half life for the hydrolysis of the maleimide moiety of **3** and for the hydrolysis of both the imide moieties in hydrogel **3**.

Compound	k_{ob} (s^{-1}) × 10^{-6}	t ½ (h)	k'_{ob} (s^{-1}) × 10^{-6}	t ½ (h)	pH
2 (sol)	7.0±0.19	27.5	-	-	6.6
2 (sol)	14±0.16	13.7	-	-	7.2
3 (sol)	7.2±0.66	26.7	67±0.5	2.9	6.6
3 (sol)	15±0.48	12.8	130±13	1.5	7.2
3 (sol)	-	-	4.3±0.27	45	6.6
3 (sol)	-	-	6.3±0.27	31	7.2

Water Gelating properties of 2 and 3. The gelation ability of **2** and **3** was determined using the stable-to-inversion-of-the container method (Table 2 and Figure 1).[11] Both **2** and **3** are not readily soluble in pure water and alkaline solutions of sodium phosphate were used to dissolve the compounds. Acidification of these solutions induces the formation of a gel suspension that becomes transparent by heating at 50 ºC and yields an hydrogel upon cooling at 25 ºC (Figure 1).

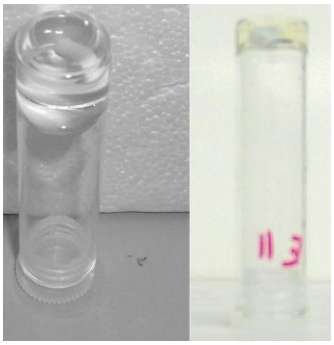

Figure 1. Pictures of self-supporting hydrogel **2** (left) and hydrogel **3** (right) in an inverted vial. Both hydrogelators where dissolved up to their CGC in 80 mM phosphate buffer pH 8.4 to give a final pH of 4.3 (for hydrogelator **2**) or pH 6.0 (for hydrogelator **3**). The magnetic bar of 2 mm entrapped within the hydrogels qualitatively shows their rigidity

The minimum gelation concentration (CGC) is pH dependent for both compounds. Changes in CGC are observed in the pH range 2.0-7.4, and can therefore be attributed to the presence of the ionisable carboxylic groups (Table 2). While the CGC values decrease at acidic pHs for both **2** and **3**, the CGCs of **3** are much lower than the CGCs of **2** at any of the pHs tested. The pKa for the carboxylic groups of structurally related compounds such as **2** and **3** is assumed to be similar in the solution state (i.e. around 340) and in first approximation in the gel state.[10] At high pHs where all the carboxylic groups are ionised the difference in CGCs is easily explained in terms of total charge and thus solubility of the compounds: **2** has a net charge of -2, while **3** has a net charge of -1. However, the differences in CGCs are maintained also for low pHs where it is reasonable to assume a similar extent of ionization (and therefore similar charge) for both gelators. [10] This result shows that the presence of the additional NAC moiety makes **2** more soluble than **3**, regardless of the protonation state of the carboxylic groups.

Transmission electron microscopy (TEM) revealed the formation of fibrillar aggregates for both hydogelators (Figure 2). The fibers are entangled and undergo splitting and overlapping in some areas of the micrographs. This arrangement of the fibers is consistent with a possible mechanism for the formation of cavity and subsequent entrapment of the water molecules that leads to gelation and that is a typical feature of the assembly of LMWG. [1,2,4-7] Whilst the morphology of the aggregates was similar, the distribution of fibers width appears to be different for the two gelators. In aggregates of **2**, 67% of the total fibers shows a 8-11 nm width and are formed by the lateral assembly of thin fibers of 4-6 nm width (Figure 2C). In the aggregate of **3**, there are no fibers with width above 8 nm and narrow fibrils of 4-5 nm width represents nearly 50% of the total fibers (Figure 2C). Since both gelators were analyzed at concentration corresponding to half the CGC, the observed difference in width distribution is consistent with **3** being a smaller molecule that yields narrower assemblies than 2.

Table 2. CGC values for gelators **2** and **3** (in mmol/l and % wt in brackets) at different pHs. The hydrogels were obtained at the pH listed in the table by acidification of solutions of **2** and **3** in 80 mM phosphate buffer pH 6.2-8.4 and were observed approximately 10 minutes (hydrogel **2**) and 20 minutes (hydrogel **3**) after formation of the solution phase.

Gelator	pH 7.4	pH 6.0	pH 4.5	pH 2.0
2	100 [5.5]	80 [4.8]	30 [1.8]	12.5 [0.92]
3	15 [0.86]	10 [0.57]	2.5 [0.14]	1.5 [0.10]

.

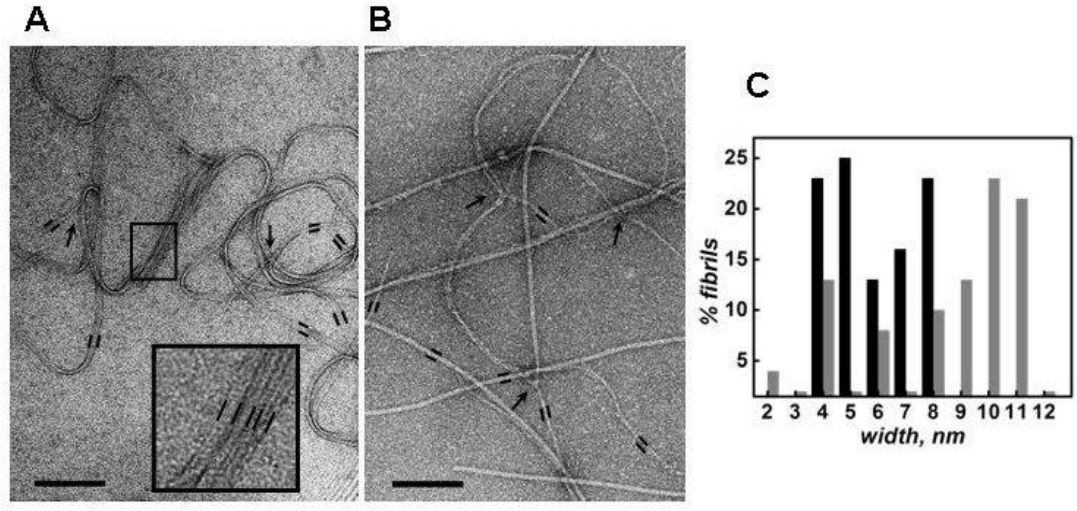

Figure 2. TEM images of hydrogel **2** (A), hydrogel **3** (B) and histograms (C) of the fibers width frequency distribution of both hydrogels (grey bars for gel **2** and black bars for gel **3**). In (A) and (B) the width of some of the fibers is marked by black bars and black arrows point to regions of splitting of the fibers. In A, the black box contours an area of fibers that are laterally assembled, this area is further magnify at the bottom of the micrograph. The scale bar is 100 nm

Multistimulus responsiveness of hydrogels 2 and 3. The gel-sol transition of **2** and **3** can be triggered by changes in temperature, pH and by the presence of a reducing agent.

Reversibility in response to heat was observed for both hydrogelators by the stable-to-inversion-of-the container method and it was studied by changes in the absorbance of the gels upon heating and cooling to accurately determine the gelation temperature (Figure 3 and Figure 5S). The hysteresis observed for hydrogel 2 indicates that gelation is thermally reversible and kinetically controlled. For **3**, the hydrogel obtained after the cooling cycle showed an absorption at 330 nm higher than before the melting cycle suggesting thermal degradation (Figure 3B). The Uv/vis spectrum of the solution obtained by dilution of the hydrogel after the melting/cooling cycle showed a an increase of the absorption in the 280-320 nm region relative to the spectrum of the gel before the melting consistent with hydrolysis of the imide moieties of **3** as observed in the study of the kinetics of hydrolysis of **2** and **3** in solution (see above) (Scheme 1S).[41] The presence of these additional carboxylic groups increases the solubility of the hydrolyzed mixture and it is consistent with the observed increase in CGC of 3 after the heating-cooling cycle.[42]

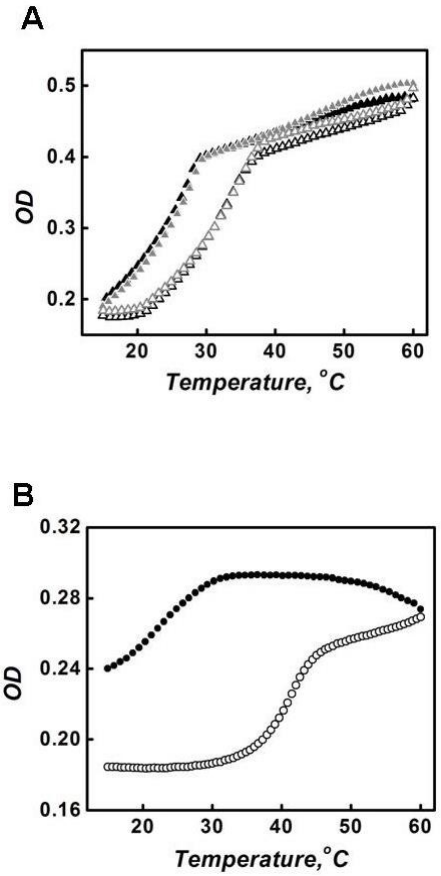

Figure 3. Thermoreversible gel-sol transitions of hydrogel **2** (A) and hydrogel **3** (B) monitored by optical density changes at 366 nm and 370 nm respectively. Empty symbols represent the melting cycle and filled symbols the cooling cycles. In A) the two hysteresis cycles corresponds to 30 mM hydrogelator **2** in 80 mM phosphate buffer pH 4.5 before (black symbols) and after consecutive addition of DTT and H_2O_2 (grey symbols). In B) 15 mM hydrogelator **3** in 80 mM phosphate buffer pH 6.5 was used to collect the data.

In the melting transition of the two hydrogels and in the cooling transition of hydrogel **2**, sloping baselines were observed. For hydrogel **3** these baselines can be attributed to the irreversible hydrolytical degradation of the gelator, but for hydrogelator **2** such degradation was not observed. The sloping baselines were therefore attributed to structural changes occurring within the residual fibrillar assemblies of the melted hydrogel. Similar baselines are also observed in the unfolding of proteins induced by denaturants or temperature and they are believed to result from residual structure in the unfolded state or non cooperative effects such as the aggregation of hydrophobic surfaces exposed to the solvent.[43]

Both hydrogelators showed pH responsive behavior attributed to the ionization of the carboxylic moieties: changing the pH of the solutions from alkaline to acidic triggered the transition to hydrogel and the subsequent addition of a base to the hydrogel induced complete dissolution allowing the reversible switching from hydrogel to solution to be controlled by changes in pH. The pH reversibility was clearly observed by the stable-to-inversion-of-the container method for both hydrogelators.

A pH dependent hydrogel to solution transition, although a non-reversible one, could also be triggered by the hydrolysis of the imide groups of hydrogelator **3**. Samples of hydrogel **3** (15 mM) at pHs 6.0, 7.0 and 8.0 undergo transition to solution in approximately 7 days, 3 days and 12 hours respectively, as observed by the stable-to-inversion-of-the container method. The kinetic of hydrolysis of **3** in the hydrogel state at pH 6.6 and 7.2 was quantified by following the changes in the UV/Vis spectrum of **3**, diluting aliquots of the hydrogel below the CGC at different time intervals (Figure 6S and Table 1). Similar to what is observed in solution, the hydrolysis in the hydrogel is pH dependent but more than an order of magnitude slower. Less than 20% of hydrolyzed **3** is observed after 10 hours from preparation of the gel at the pH values monitored in contrast to quantitative hydrolysis observed in solutions of **3** (Figure 6S). This result shows that the imide moieties are protected from hydrolysis in the hydrogel state and it is consistent with these groups being in a more hydrophobic environment relative to the solution state. Such protective modulation of the hydrolysis reaction is also observed for succinimide groups within the folded state of proteins and it is attributed to different exposure of these groups to the aqueous environments in addition to other structural factors.[44] The stability to hydrolysis observed for hydrogel **2** relative to **3** is explained in terms of pH dependence of the hydrolysis reaction: at the acidic pH that induces gelation of **2** the hydrolysis reaction is extremely slow (Table 1).Although the gel-sol transition triggered by hydrolysis is irreversible, the timescale makes it a potentially useful trigger for drug release applications as shown by experiment of release of bioactive substances from hydrogelator **3** (see below).

The gel-sol transition of **2** can be reversibly tuned using thiol/disulfide exchange as the redox reaction (Scheme 2A). A gel-sol transition was observed by the vial-inversion method 30 minutes after the addition of the reducing agent dithiothreitol (DTT) to hydrogelator **2** (Figure 4A).

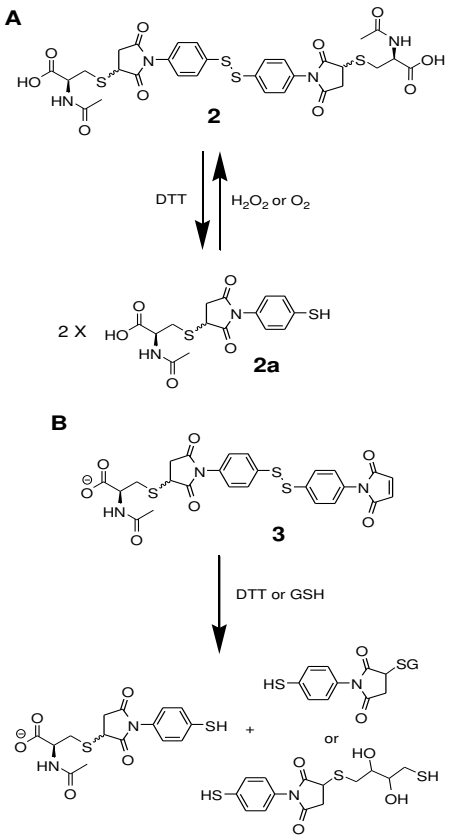

Scheme 2. A) Conversion of **2** into **2a** by reductive cleavage initiated by addition of excess DTT and re-oxidation of **2a** to **2** initiated by addition of excess H_2O_2 or by atmospheric oxygen. B). Reaction of **3** with an excess of the reducing agents DTT or GSH.

The transition to solution is attributed to the reductive cleavage of hydrogelator **2**, which yields the non-gelating thiol **2a** (Scheme 2A), as demonstrated by mass spectroscopy analysis of an aliquot of the gelator at different time intervals after addition of DTT (Figure 4B and C). Addition of an excess of the biological oxidant H_2O_2 over a DTT treated sample resulted in the reverse sol to gel transition, attributed to re-formation of hydrogelator 2 by oxidation of thiol **2a** (Scheme 2A, Figure 4C).[45] The vial inversion experiment showed that the sol-gel transition was complete in 30 minutes. An aliquot of the hydrogel was analyzed by LC-MS, confirming that **2** had been almost completely regenerated after this time (Figure 4B and C). Other higher oxidation state sulfur compounds, that can form by reaction of thiol **2a** with H_2O_2 and that could potentially lead to degradation of **2** were not detected (Figure 4C). Furthermore, the hydrogel obtained after oxidation has a melting and cooling cycle identical to the hydrogel before the redox cycle showing that the process is reversible (Figure 3A). Re-formation of the hydrogel followed also atmospheric oxidation of thiol **2a**. However in this case the sol to gel transition took up to 12 hours, as showed by the vial inversion experiment.

Like **2**, hydrogelator **3** contains a disulfide bond that can undergo reductive cleavage. However since **3** is a non-symmetric disulfide it is not possible to re-generate pure **3** after oxidation of the reduced mixture as this reaction would lead to the formation of a mixture of disulfides and thus to a decrease of the CGC of **3**.[46] Moreover the thiols formed by reduction of 3 can react with the maleimide moieties leading to the formation of further side products (Scheme 2B).[37] However, while the reductive cleavage of **3** is irreversible it initiates a gel-sol transition which can be used as an effective trigger for the release of drugs entrapped in the hydrogelator (see below).

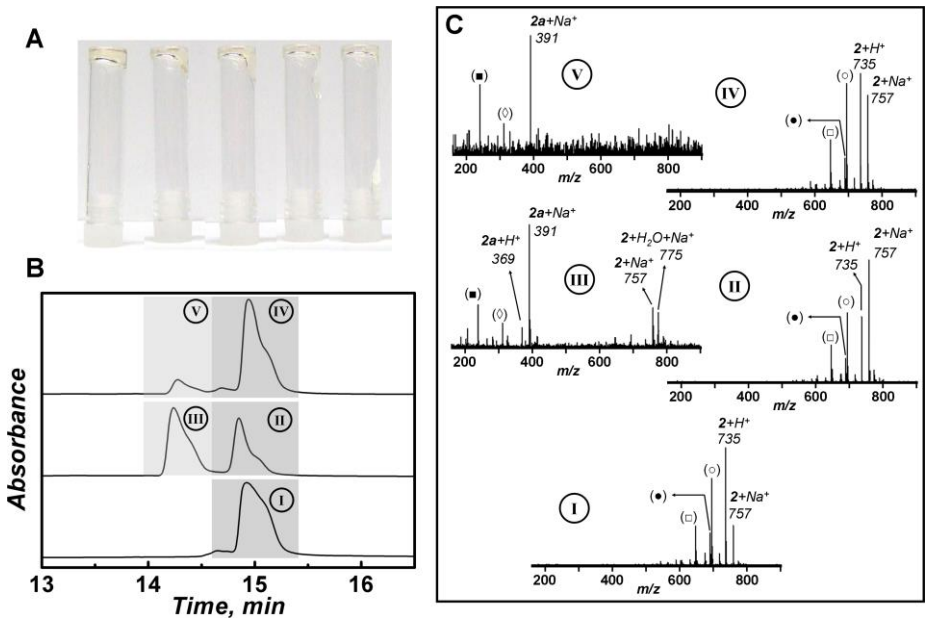

Figure 4. A) Seven photos of inverted hydrogel **3** taken 10 minutes (first test tube on the left) and subsequently at intervals of approximately 1 minute after addition of DTT. B) UV absorption HPLC traces (detector at 250 nm) from the HPLC-MS experiments of an aliquot of **2** in the hydrogel state (lower trace), and the same sample turned into a sol 30 min after addition of DTT (middle trace) and the hydrogel resulting from the addition of H_2O_2 over the DTT treated solution (30 min after H_2O_2 addition) (upper trace). The shaded areas labelled with roman numerals yield the corresponding MS spectra depicted in C. C). MS of the corresponding shaded areas of the HPLC chromatogram. Only the masses of the peaks corresponding to the major products **2** and **2a** are shown for clarity Satellite peaks labelled with symbols corresponds to fragments of the major products **2** and **2a.** The masses and structures of these fragments are shown in Scheme2S

Release of bioactive substances from hydrogelator 3. Gelators that can be formed under biocompatible conditions and are responsive to biologically relevant stimuli are good candidates for the development of drug delivery systems.[1,12,22-25,32] We used hydrogelator **3** with entrapped vitamin B_{12} as an in vitro model to investigate the potential of **3** as a controlled release drug delivery system. Compound **3** was chosen instead of **2** because it is the best hydrogelator with a CGC ten times lower than **2** in a range of pH values that are biologically relevant (Table 2). Vitamin B_{12} was chosen as the drug because of its pharmacological importance and its spectroscopic properties that allow following release of the drug in a spectral region (550 nm) where many gelators, including **3**, are optically transparent.[24,32] Three different stimuli were used to control the release of the vitamin from the hydrogel: changes in pH, the spontaneous hydrolysis of the gelator and the reductive cleavage of **3**'s disulfide bond initiated by the addition of gluthatione (GSH), a thiol that regulates the redox balance in cells (Figure 5).[45]

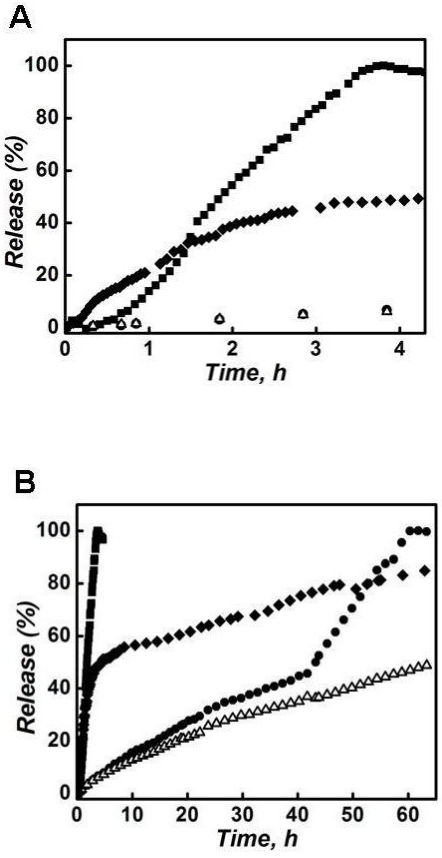

Figure 5. Initial stages (A) and overall time course (B) of vitamin B_{12} release (5% mol in the gel) from hydrogel **3** (15 mM) triggered by three different stimuli: addition of a solution 1 mM of GSH , pH 7.4 (and hydrogel-vitamin at pH 7.4)(■), a pH change (hydrogel-vitamin at pH 5.3 and surrounding buffer at pH 7.4)(◆) and spontaneous hydrolysis of the hydrogelator at pH 7.4 (●) (both hydrogel-vitamin and surrounding solution at pH 7.4). The pH 6.0 curve (△), where no hydrolysis-induced release is observed during the monitored period, shows the release due purely to the dissolution of the hydrogel in the surrounding buffer. Note that the rate of release between the 10th and 40th hour approximately is very similar for all the stimuli (except reduction,■), and is attributed to the spontaneous dissolution of the hydrogel.

The release of vitamin was followed by continuous spectrophotometric assay of a solution that was into contact with the hydrogel and that was buffered at the physiological pH value of 7.4 or at pH 6.0, (See experimental section and Figure 7S, for details of the experimental set up). We found that irrespective of the external stimulus, the release of vitamin is accompanied by the dissolution of the hydrogel by dilution in the surrounding buffer, consistent with a strong affinity of the relatively hydrophobic drug for the hydrogel **3**. Release triggered by pH changes was achieved by preparing the hydrogel with entrapped vitamin at lysosomal pH (5.3) and using as the release solution buffer at pH 7.4.[47] The release of vitamin begins upon contact with the high pH buffer. The rate of both vitamin release and gel dissolution is approximately constant for the first two hours. During this time, around 50% of the vitamin is released (Figure 5A). After this time the rate of vitamin release decreases rapidly and levels off to a value more than 30 fold slower, which is maintained until total dissolution of the gel, approximately 60 hours after the start of the experiment (Figure 5B). The fast initial release phase is consistent with a structural change of the gel induced by the exhaustive de-protonation of **3** upon change of the pH. The second slower release phase is on the other hand attributed to the dissolution of the gel, once the gel reaches the pH of the external buffer. This interpretation is supported by the observation that the rate of release observed in the second phase is similar to the rate of release observed in absence of an external stimulus (see below and Figure 5).

Release triggered by spontaneous hydrolysis was achieved by preparing the hydrogel with entrapped vitamin and the surrounding buffer at the same pHs (7.2 and 6.0, Figure 5). At pH 7.2, the release is biphasic: in the initial phase it is similar to the release observed at pH 6.0 (Figure 5) and was therefore attributed to the process of dissolution of the hydrogel. After this phase that last approximately 40 hours when nearly 40% of the vitamin is released, the rate suddenly increases 4 fold and in this second phase the remaining 60% of the vitamin is released. The onset of the second faster phase is attributed to the presence of a critical amount of the more soluble hydrolyzed hydrogelator that increases the rate of gel dissolution relative to the first phase of release. At pH 6.0 on the other hand the rate of release is approximately constant and similar to that of the first phase of release observed at pH 7.2, and does not change for the period of time monitored (60 h), consistent with the slower hydrolysis of the hydrogel at lower pH.

Release of vitamin B_{12} triggered by the reductive cleavage of **3**'s disulfide bond was achieved by addition of GSH to the buffer surrounding the hydrogel, with the hydrogel and the buffer both at pH 7.2. All the vitamin is released between 3-4 hours after addition of GSH in a single phase with a rate increase of 30 fold relative to release induced by the dissolution of the hydrogel in the surrounding buffer. This increase in the rate of vitamin release is attributed to the reductive cleavage of the disulfide bond of **3** that leads to a mixture of thiols more hydrophilic and therefore more readily soluble in the surrounding buffer relative to hydrogel **3** (Scheme 2 B).

Conclusion

Our limited ability to predict the assembly properties in water of novel compounds makes it difficult to design multi-responsive LMWHs. As a consequence, the design of many LMWHs is typically based on the functionalisation of structural motives that are known to assemble in gel-forming fibrils and are usually responsive to a single stimulus. The gelators described in this work, while discovered rather than designed, suggest a general strategy to achieve multiresponsiveness with minimal disruption of the hydrophobic-hydrophilic balance of the molecule: to introduce hydrophobic (i.e. disulfide bonds) and hydrophylic (i.e. carboxylic

moieties) stimuli-responsive moieties in the appropriate parts of the molecule. The ability of LMWH **2** to gelate water can be controlled by at least **3** stimuli: changes in pH, temperature and the presence of specific red-ox agents (Figure 6), showing that **2** is an excellent blueprint for the development of smart materials. LMWH **3** on the other hand shows reversible gel-to-sol transitions upon pH and temperature changes, but also a non-reversible one due to hydrolytic degradation of the imide moieties (Figure 6). **3** has also a remarkable low CGC at physiologically relevant pHs. Therefore **3** is an excellent model of drug release vehicle, with a release rate that can be modulated by the presence of three different stimuli. It is worth noting that the development of **2** and **3** into derivatives that are more efficient for drug release or for other soft nanotechnology applications should be relatively straightforward thanks to their modular structures that is easily amenable to molecular design. There are obvious points of this structure that can be modified in the search for novel gelators: other thiols or ligands bearing amines can be added to the maleimide moieties and different aromatic disulfides can be appended to the maleimide group. Previous work has shown that these aromatic disulfides undergo reversible photocleavage and we anticipate that this could provide a further tool to expand the responsiveness and hence applicability of these gelators. Current work in our lab is focusing on these developments.

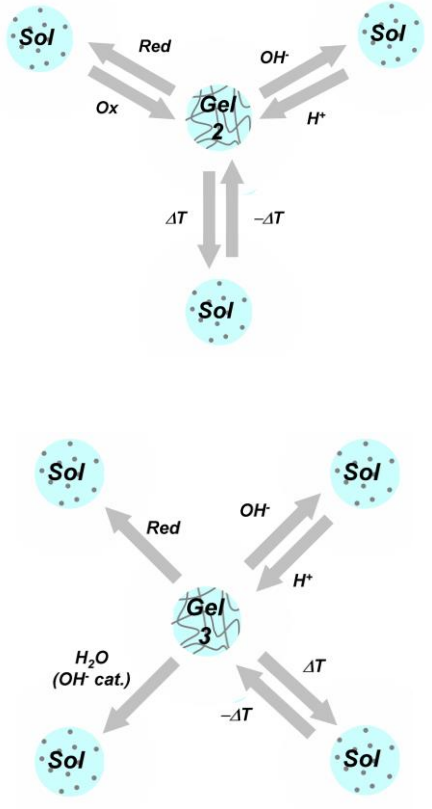

Figure 6. Stimuli responsivenes of gel **2** and **3** characterized in this work.

Experimental Section

Materials and Methods. Chemicals and solvents were obtained from commercial sources and used without further purification. ^{1}H and ^{13}C NMR spectra recorded on a Bruker AMX400 . All chemical shifts are quoted in ppm and spectra were referenced to the residual solvent signal. All buffers were filtered through a 0.2 μm cellulose membrane (Amicon) and the pH values given are not corrected for the deuterated solutions.Positive electrospray (ES^+) mass spectra were recorded on a Fison VG Platform using a quadrupole detection system. UV-vis absorbance spectra were recorded with a Thermoelectron Corporation UV1 Thermospectronic UV-vis spectrometer and with a Varian Cary 3 spectrophotometer equipped with a Varian Cary temperature controller for the gel melting measurements. For ES^+ mass spectroscopy (MS) analysis of hydrogel 2 after subsequent addition of DTT and H_2O_2, a Agilent 1100 series LC-MS platform equipped with a Phenomenex-Gemini C-18 (3 μm) prepacked column (20 x 4.0 mm)was used. RP-C18 preparative chromatography was performed with a Phenomenex-Jupiter Proteo (90 Å, 10 μm) prepacked colum (150 x 21.2 mm) connected to a Gilson 300 series HPLC setup equipped with a quaternary gradient pump (flow rate: 10 mL min^{-1}), and a UV/Vis detector set at λ = 220 nm.

Synthesis of 2 and 3. The procedure for the synthesis of **2** and **3** was modified from a previously reported procedure [36] as follow: a solution of NAC (0.58 g, 3.60 mmol) was added slowly and under vigorous stirring to a solution of **1** (1 g, 2.45 mmol) in MeCN. The reaction mixture was left overnight stirring under nitrogen. The solvent was then removed under reduced pressure and the resulting hydrogel was dissolved in water/dioxane = 50/50 v/v. The solvent was then removed using a freeze drier to give a white residue (1.5 g). This solid was dissolved in 10 mL of DMF and was purified by RP-HPLC eluting with 0.1% TFA-MeCN/0.1% TFA–H_2O with the following gradient: 0-15 min, 50% MeCN, 15-20 min, 50→20% MeCN, 20-30 min 20→50% MeCN. Fractions corresponding to **2** (tr = 15 min) and **3** (tr = 20 min) were collected and concentrated under reduced pressure. Residual water was removed with a freeze drier to give pure **2** (0.9 g, 50 % yield) and **3** (0.42 g, 30% yield). For the characterization of **2** and **3** see Supplementary Material.

Hydrolysis Measurements. Stock solutions of **2** (2.5 mM) or **3** (2.5 mM) in 50 mM phosphate buffer pH 6.6, 7.2, and 7.7 were diluted in the same buffers down to 120 μM (**2**) and 41 μM (**3**). The diluted solutions were maintained at 25 ºC and UV/ Vis. spectra were recorded in the 250-450 nm region using the automated acquisition of the scanning kinetics program of the spectrophotometer. Rate constants were derived by fitting the spectral data to the relevant kinetic models using SPECFIT 3.0.[48] For hydrolysis of **2**, an irreversible one step kinetic model of the type A→B was used whilst for hydrolysis of **3** an irreversible two step consecutive model of the type A→B→C was used. In these models only the following species are considered: unmodified (A), single hydrolyzed (B) and hydrolyzed (C) specie and it is assumed that hydrolysis of the succinimide rings of **2** and imide rings of **3** occurs independently given the distance between the two rings (see Supplementary information and Figure 4S for further details).[10] Hydrolysis measurements of hydrogel **3** were carried out as follow: two samples of hydrogel **3** were prepared in 80 mM phosphate buffer pH 6.6 and pH 7.2 and then aliquots of the hydrogels were withdrawn and transferred in a vial containing the same buffers and diluted down to 41 μM. These solutions containing hydrogel were sonicated for five minutes and aliquots of the supernatant were withdrawn for UV/Vis measurements at different time intervals from preparation of the hydrogels (1-47 hours). The absorbance of these solutions was compared with the UV/Vis spectra recorded to monitor hydrolysis of 3 below the CGC using SPECFIT 3.0.[48] This allowed determining the percentage of hydrolyzed **3** in gel **3** from the known percentages of hydrolyzed species determined using SPECFIT for solution of **3** (e. g. below the CGC) (see Figure 6S).

Gelation. In a typical experiment, **2** (0.9-5 % w/v) and **3** (0.1-09 % w/v) were dissolved in 80 mM phosphate buffer pH 8.4 (for **2**) and pH 7.4 or 6.2 (for **3**) in a vial equipped with a magnetic stirrer. To this solution small aliquots (1-5 μL for 1 mL) of HCl 5-10 M were added up to formation of a precipitate. This precipitate was dissolved by heating (approximately 50ºC) and the warm solution was left to cool at r.t.. The vial was then inverted to test for gelation and if the system was not self supporting, more HCl was added and the above procedure repeated. The final pH of the hydrogels was then measured.

Electron microscopy. Hydrogel **2** (CGC 30mM, pH 4.5) and **3** (CGC 15 mM, pH 7.4) prepared in 80 mM phosphate buffer were melted by heating at 50 ºC and aliquots of the warm solutions were diluted in distilled water to 15 mM for **2** and 7.5 mM for **3**. 5 μl of these solutions were loaded on freshly discharge carbon coated grids, blotted with filter paper and negatively stained with 2% (w/v) uranyl acetate. Low dose images were recorded on a 200 keV F20 microscope (FEI) at magnifications of 29,000 x, 50,000 x and 80,000 x on Kodak SO-163 film with a defocus range of 1–3 μm. Micrographs were digitized on a Zeiss SCAI scanner at a pixel size of 14 μm corresponding to 4.82 Å, 2.80 Å and 1.75 Å pixel size on the specimen for magnifications of 29,000 x , 50,000 x and 80,000 x respectively. The width of approximately 100 fibrils for each hydrogelator was determined using the measure distance and angles tool of GIMP 2.6.[49] Only segments of fibrils that appeared straight and flat were selected for the measurements.

Gel Melting Temperature Measurements. Hydrogel **2** (30 mM) and **3** (15 mM) prepared in 80 mM phosphate buffer pH 4.5 and 6.5 respectively were melted at approximately 50 ºC and aliquots of 200 μL were transferred to a quartz cuvette with a 1 mm path length and allowed to cool at r.t.. For gel **2** the sample was first heated at 60 ºC and then allowed to cool to 15 ºC. The cooled sample was then re-heated to 60 ºC. The rate was 2 ºC/min for both cycles and the absorbance of the sample at 366 nm was recorded. For gel **3**, the sample was first subjected to a melting cycle from 15 to 60 ºC and then to a cooling cycle from 60 to 15 ºC. The rate was 3 ºC/min for both cycles and the absorbance of the sample at 370 nm was recorded.

Reversible tuning of gelation by pH changes. 1 ml of hydrogel **2** (30 mM, pH 4.5) was melted to 50 ºC under stirring and to the solution, aliquots (1-5μL) of NaOH 1-5M were added up to complete dissolution of the gel phase (pH 5.2, NaOH 6 mM). To the cold solution aliquots of HCl 1M were added under stirring and up to formation of the gel phase (pH 4.5, HCl 5mM) as tested by the vial inversion method.[11] The above procedure was repeated 3 times and the resulting gel was subjected to a cycle of melting and cooling as described in Gelation Temperature Measurements. A similar procedure was used to test pH reversible gelation of 3: 1 mL of gel **3** (2.5 mM in 80 mM phosphate buffer pH 4.5) was melted and to the solution 3μL of NaOH 1M were added under stirring. The cold solution was then added of aliquots of HCl 1M up to formation of the gel phase as test by the vial inversion method. This procedure was repeated three times and a hydrogel was formed for each cycle of the pH switch. This indicates that hydrolysis of hydrogelator **3** did not take place during the course of the pH switch probably due to the slow kinetic of this reaction relative to the time scale of the pH switch experiment.

Reversible tuning of gelation of 2 by redox reactions. Gelator **2** (30mM) in 80 mM phosphate buffer pH 4.5 was melted by heating it to 50 ºC in a water bath. An aliquot (10 μL) was diluted into 500 μL of water and was immediately subjected to LC-MS analysis (see Figure 4C). To the remaining sample, a solution of DTT 5M in H_2O was added to yield 36 mM DTT in the sample. An aliquot of 130 μL was transferred to a vial and then inverted to take pictures at intervals of 1 minute. After 30 minutes from DTT addition the hydrogel had turned to solution. 10 μL of this solution were diluted into 500 μL of water and immediately subjected to LC-MS analysis (see Figure 4C). To the remaining sample a solution of H_2O_2 8.5M in H_2O was added to yield 42 mM H_2O_2.in the sample. After 30 minutes the sol had become gel again. 10 μL of the gel were diluted into 500 μL of water and immediately subjected to LC-MS analysis (see Figure 4). The remaining gel sample was subjected to a cooling and melting cycle as described above for Gel Melting Temperature Measurements (see Figure 3A). The timescale and reproducibility of the redox switch were assessed by repeating the above procedure 3 times.

Release experiments: In a typical experiment, 55 μl of melted hydrogel **3** (30 mM in phosphate buffer 160 mM at the required pH) were mixed with 55 μl of vitamin B_{12} 0.76 mM in water (obtained by dilution of a 7 mM stock) to yield a solution 15 mM in **3** and 0.38 mM in vitamin B_{12} in phosphate buffer 80 mM at the required pH. 30 μL of this solution were quickly transferred into a volume-displacement plastic pipette tip that had had the thin end cut off so that the diameter of the aperture of the end of the pipette tip was identical to the diameter of its cylindrical section. After the solution became gel upon cooling at r.t., the pipette tip containing the vitamin loaded hydrogel was place on top of a quartz cuvette in contact with 1mL of 80 mM phosphate buffer at the appropriate pH and UV/Vis spectra of the surrounding buffer were recorded up to 80-100% release of vitamin (see figure 7S). The pH of the stock hydrogel loaded with vitamin B_{12} and supernatant buffers were identical except for measurements of release triggered by a pH change. For these experiments hydrogel **3** was prepared in 80 mM phosphate buffer pH 5.3 and the same solution buffered at pH 7.4 was used as the supernatant. The pH of the hydrogel and the supernatant for measurements of release triggered by hydrolysis were 6.0 and 7.4. For measurements of release triggered by a redox reaction hydrogel 3 was prepared in 80 mM phosphate buffer pH 7.4 and the same buffer added of 1 mM glutathione was used as the supernatant. During all the experiments the pink color of the remaining gel inside the tip did not change, qualitatively showing that the release of the vitamin required the dissolution of the hydrogel.

Acknowledgements

We thank Robert Hanson and Simon Thorpe (The University of Sheffield) for technical assistance in RP-HPLC, Dr. Philip Lowden (Birkbeck University of London) for the use of mass spectrophotomer, Prof. Steve Caddick (University College London) for the use of NMR facilities, Prof. Helen Saibil (Birkbeck University of London) for the use of EM facilities, the BBRSC and the Wellcome Trust for funding.

[1] M. de Loos, B. L. Feringa, J. H. van Esch, *Eur. J. Org. Chem.* **2005**, 3615-3631.

[2] L. A. Estroff, A. D. Hamilton, *Chem. Rev.* **2004**, *104*, 1201-1217.

[3] D. J. Abdallah, R. G. Weiss, *Adv. Mater.* **2000**, *12*, 1237-1247.

[4] L. A. Estroff, L. Leiserowitz, L. Addadi, S. Weiner, A. D. Hamilton, *Adv. Mater.* **2003**, *15*, 38-42.

[5] R. J. Mart, R. D. Osborne, M. M. Stevens, R. V. Ulijn, *Soft Matter* **2006**, *2*, 822-835.

[6] W. H. Binder, O. W. Smrzka, *Angew. Chem., Int. Ed.* **2006**, *45*, 7324-7328.

[7] K. S. Moon, H. J. Kim, E. Lee, M. Lee, *Angew. Chem., Int. Ed.* **2007**, *46*, 6807-6810.

[8] E. F. Banwell, E. S. Abelardo, D. J. Adams, M. A. Birchall, A. Corrigan, A. M. Donald, M. Kirkland, L. C. Serpell, M. F. Butler, D. N. Woolfson, *Nature Mater.* **2009**, *8*, 596-600.

[9] M. Suzuki, K. Hanabusa, *Chem. Soc. Rev.* **2009**, *38*, 967-975.

[10] K. J. C. van Bommel, C. van der Pol, I. Muizebelt, A. Friggeri, A. Heeres, A. Meetsma, B. L. Feringa, J. van Esch, *Angew. Chem., Int. Ed.* **2004**, *43*, 1663-1667.

[11] F. M. Menger, K. L. Caran, *J. Am. Chem. Soc.* **2000**, *122*, 11679-11691.

[12] J. C. Tiller, *Angew. Chem., Int. Ed.* **2003**, *42*, 3072-3075.

[13] A. R. Hirst, B. Escuder, J. F. Miravet, D. K. Smith, *Angew. Chem., Int. Ed.* **2008**, *47*, 8002-8018.

[14] Z. Yang, G. Liang, B. Xu, *Acc. Chem. Res.* **2008**, *41*, 315-326.

[15] D. Kamarun, X. W. Zheng, L. Milanesi, C. A. Hunter, S. Krause, *Electrochim. Acta* **2009**, *54*, 4985-4990.

[16] N. M. Sangeetha, U. Maitra, *Chem. Soc. Rev.* **2005**, *34*, 821-836.

[17] J. J. D. de Jong, L. N. Lucas, R. M. Kellogg, J. H. van Esch, B. L. Feringa, *Science* **2004**, *304*, 278-281.

[18] X. B. Zhao, F. Pan, H. Xu, M. Yaseen, H. H. Shan, C. A. E. Hauser, S. G. Zhang, J. R. Lu, *Chem. Soc. Rev.*, *39*, 3480-3498.

[19] G. John, P. K. Vemula, *Soft Matter* **2006**, *2*, 909-914.

[20] R. G. Ellis-Behnke, Y. X. Liang, S. W. You, D. K. C. Tay, S. G. Zhang, K. F. So, G. E. Schneider, *Proc. Natl. Acad. Sci. U. S. A.* **2006**, *103*, 5054-5059.

[21] G. A. Silva, C. Czeisler, K. L. Niece, E. Beniash, D. A. Harrington, J. A. Kessler, S. I. Stupp, *Science* **2004**, *303*, 1352-1355.

[22] Z. Yang, G. Liang, Z. Guo, Z. Guo, B. Xu, *Angew. Chem., Int. Ed.* **2007**, *46*, 8216-8219.

[23] F. Plourde, A. Motulsky, A. C. Couffin-Hoarau, D. Hoarau, H. Ong, J. C. Leroux, *J. Control. Release* **2005**, *108*, 433-441.

[24] S. Ray, A. K. Das, A. Banerjee, *Chem. Mater.* **2007**, *19*, 1633-1639.

[25] P. K. Vemula, G. A. Cruikshank, J. M. Karp, G. John, *Biomaterials* **2009**, *30*, 383-393.

[26] F. Rodriguez-Llansola, J. F. Miravet, B. Escuder, *Chem. Commun.* **2009**, 7303-7305.

[27] S. Kiyonaka, K. Sada, I. Yoshimura, S. Shinkai, N. Kato, I. Hamachi, *Nature Mater.* **2004**, *3*, 58-64.

[28] G. L. Liang, H. J. Ren, J. H. Rao, *Nature Chem.* **2010**, *2*, 54-60.

[29] D. Lowik, E. H. P. Leunissen, M. van den Heuvel, M. B. Hansen, J. C. M. van Hest, *Chem. Soc. Rev.*, *39*, 3394-3412.

[30] L. Frkanec, M. Jokic, J. Makarevic, K. Wolsperger, M. Zinic, *J. Am. Chem. Soc.* **2002**, *124*, 9716-9717.

[31] A. Pal, S. Shrivastava, J. Dey, *Chem. Commun.* **2009**, 6997-6999.

[32] H. Komatsu, S. Matsumoto, S. Tamaru, K. Kaneko, M. Ikeda, I. Hamachi, *J. Am. Chem. Soc.* **2009**, *131*, 5580-5585.

[33] P. Terech, R. G. Weiss, *Chem. Rev.* **1997**, *97*, 3133-3159.

[34] C. J. Bowerman, B. L. Nilsson, *J. Am. Chem. Soc.*, *132*, 9526-9527.

[35] J. D. Hartgerink, E. Beniash, S. I. Stupp, *Proc. Natl. Acad. Sci. U. S. A.* **2002**, *99*, 5133-5138.

[36] L. Milanesi, G. D. Reid, G. S. Beddard, C. A. Hunter, J. P. Waltho, *Chem. Eur. J.* **2004**, *10*, 1705-1710.

[37] L. Milanesi, C. Jelinska, C. A. Hunter, A. M. Hounslow, R. A. Staniforth, J. P. Waltho, *Biochemistry* **2008**, *47*, 13620-13634.

[38] J. Schlesinger, C. Fischer, I. Koezle, S. Vonhoff, S. Klussmann, R. Bergmann, H. J. Pietzsch, J. Steinbach, *Bioconjugate Chem.* **2009**, *20*, 1340-1348.

[39] J. Kalia, R. T. Raines, *Bioorg. Med. Chem. Lett.* **2007**, *17*, 6286-6289.

[40] J. T. Doi, M. H. Goodrow, W. K. Musker, *J. Org. Chem.* **1986**, *51*, 1026-1029.

[41] P. Knight, *Biochem. J.* **1979**, *179*, 191-197.

[42] A. R. Hirst, I. A. Coates, T. R. Boucheteau, J. F. Miravet, B. Escuder, V. Castelletto, I. W. Hamley, D. K. Smith, *J. Am. Chem. Soc.* **2008**, *130*, 9113-9121.

[43] M. A. C. Reed, C. Jelinska, K. Syson, M. J. Cliff, A. Splevins, T. Alizadeh, A. M. Hounslow, R. A. Staniforth, A. R. Clarke, C. J. Craven, J. P. Waltho, *J. Mol. Biol.* **2006**, *357*, 365-372.

[44] L. Athiner, J. Kindrachuk, F. Georges, S. Napper, *J. Biol. Chem.* **2002**, *277*, 30502-30507.

[45] M. D. Rees, E. C. Kennett, J. M. Whitelock, M. J. Davies, *Free Radical Biol. Med.* **2008**, *44*, 1973-2001.

[46] L. Milanesi, C. A. Hunter, S. E. Sedelnikova, J. P. Waltho, *Chem. Eur. J.* **2006**, *12*, 1081-1087.

[47] R. G. W. Anderson, L. Orci, *J. Cell Biol.* **1988**, *106*, 539-543.

[48] H. Gampp, M. Maeder, C. J. Meyer, A. D. Zuberbuhler, *Talanta* **1986**, *33*, 943-951.

[49] http://www.gimp.org

Received: ((will be filled in by the editorial staff))
Revised: ((will be filled in by the editorial staff))
Published online: ((will be filled in by the editorial staff))

Supplementary Material

Characterisation of 2 and 3. The HRMS (ES^+), 1H and 13C NMR of **2** in DMSO-d_6 have been reported previously.[37] In this work we report the assignment of the 1H NMR spectrum of **2** based on ^{1}H-^{1}H COSY.(Figure 1S and 2S).

The 1H NMR spectrum of **3** is identical to the 1H NMR of **2** , except for the presence of the maleimide protons signal therefore we can assign the 1H NMR of **3** based on the assignment of the 1 H NMR of **2** (Figure 3S). ^{1}H NMR (300 MHz, DMSO-d_6), δ ppm: 1.84 (s, 1.5 H), 1.86 (s, 1.5 H), 2.66 (ddd, *J*=18.27, 10.37, 4.28 Hz, 1 H), 2.91 (dd, *J*=13.65, 9.10 Hz, 0.5 H), 2.99 - 3.21 (m, 0.5 H), 3.23 - 3.34 (m, 1.5 H), 4.16 (dt, *J*=9.03, 4.45 Hz, 1 H), 4.35 - 4.55 (m, 1 H), 7.18 (s, 2H), 7.25 - 7.45 (m, 4 H), 7.57 - 7.75 (m, 4 H), 8.34 (dd, *J*=8.03, 2.41 Hz, 1 H), 12.95 (br. s, 1 H) ppm. 13C NMR of **3**: (DMSO-d_6) δ ppm: 175.75, 175.63, 174.04, 174.00, 169.69, 169.47, 169.34, 135.84, 134.79, 134.76, 131.49, 131.04, 127.99, 127.97, 127.66, 127.59, 127.40, 51.98, 51.50, 40.48, 36.19, 22.36. HRMS (ES^+): expected for $C_{25}H_{21}N_3O_7NaS_3$ $(M + Na)^+$ 594.0468, found 594.0439

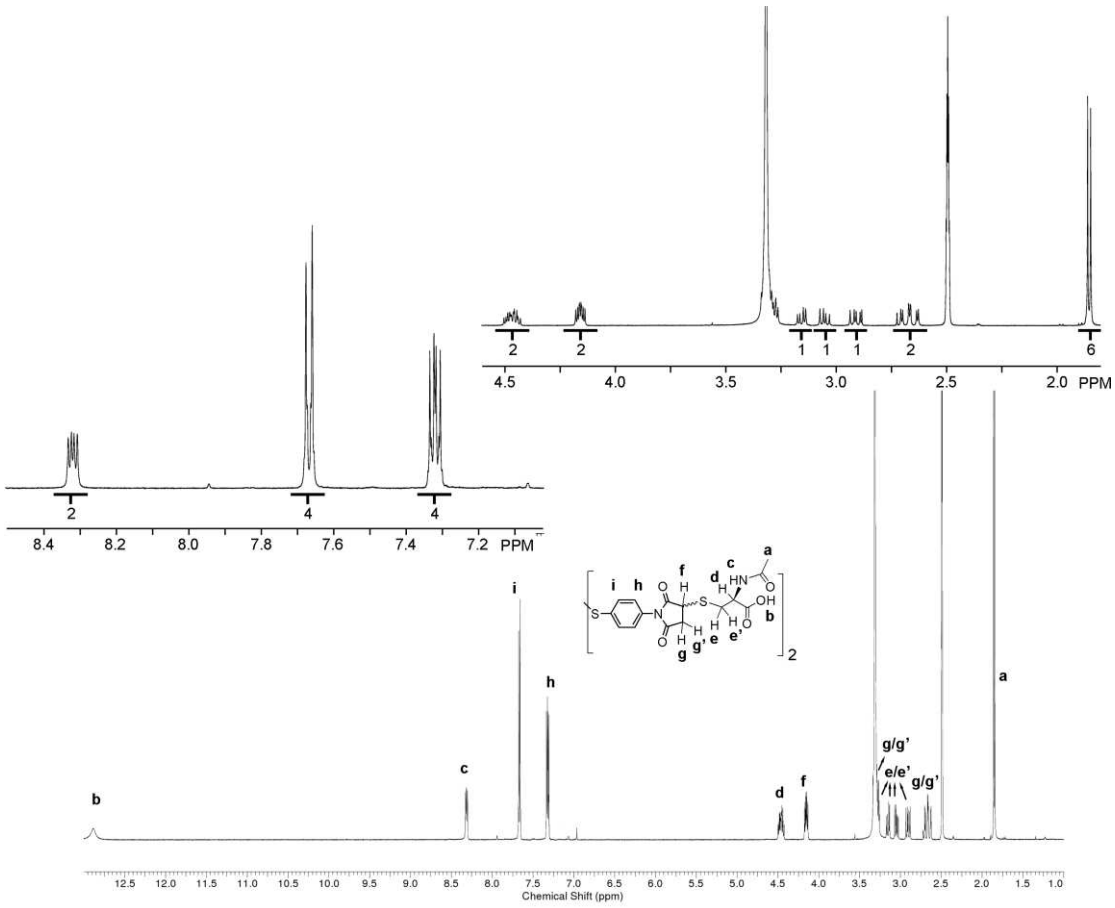

Figure 1S. 1H NMR spectrum of 2 (5mM) in DMSO-d_6 (bottom trace) and expansions of the same spectrum (upper traces). The numbers below each set of peaks are the values for the integration. Letters on top of each set of peaks refer to the assignments of the spectrum according to the labelling scheme shown on the structure of **2** (inset). For each set of peaks between 2.5 and 3.5 ppm, a double letter labelling scheme is shown to indicate that these peaks can be equally assigned to any of two diastereotopic hydrogens.

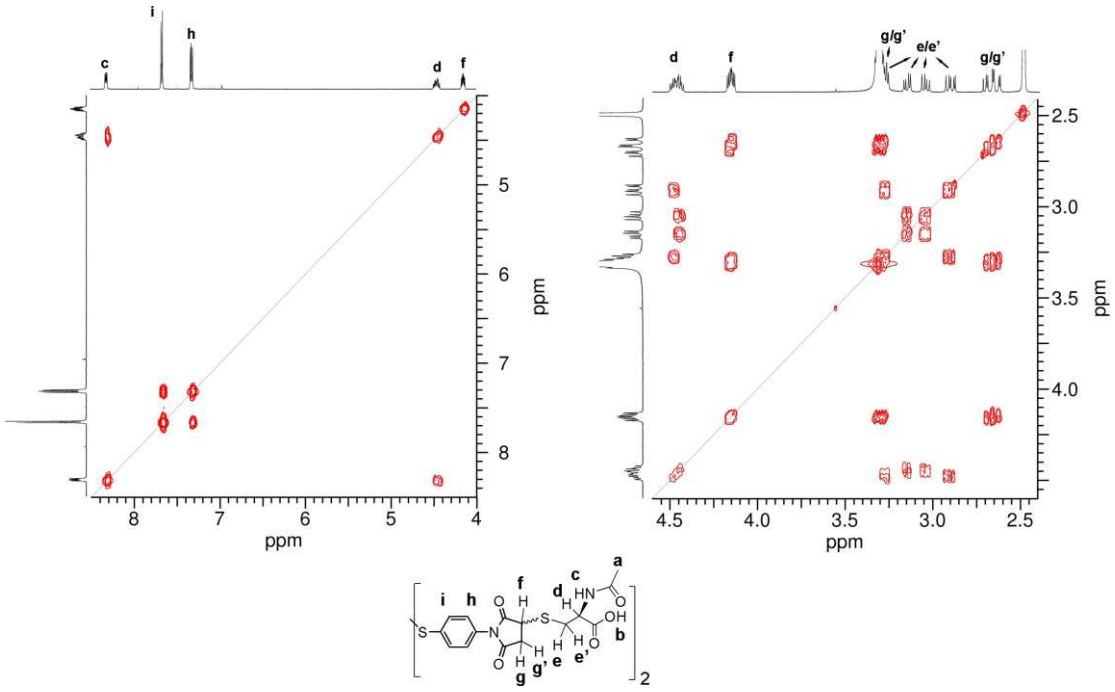

Figure 2S. 1H-1H COSY spectrum of **2** (5mM) in DMSO- d_6 (500 MHz).

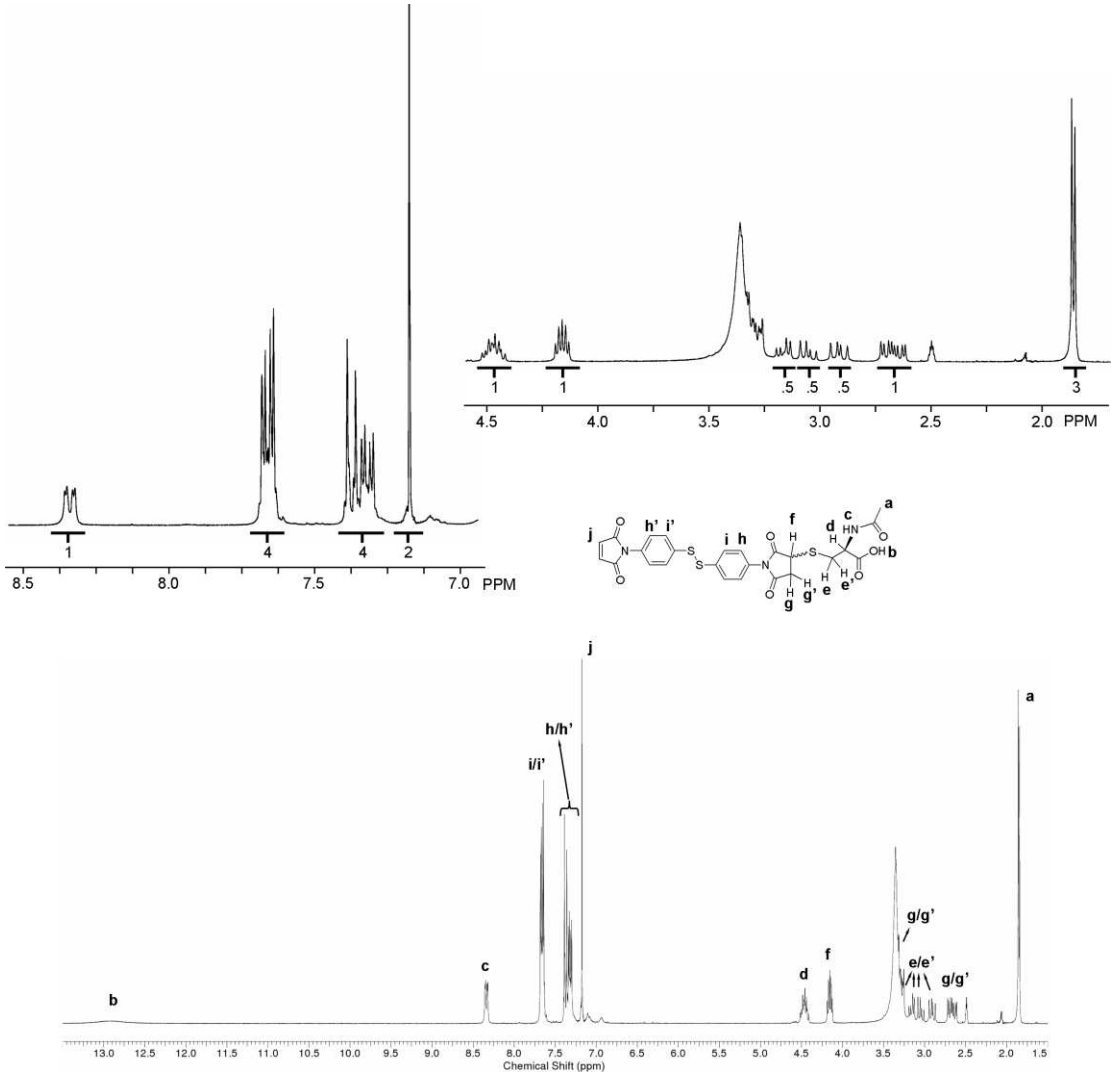

Figure 3S. 1H NMR spectrum of 3 (10 mM) in DMSO-d_6 (bottom trace) and expansions of the same spectrum (upper traces). The numbers below each set of peaks are the values for the integration. Letters on top of each set of peaks refer to the assignments of the spectrum according to the labelling scheme shown on the structure of **3** (inset). For each set of peaks between 2.5 and 3.5 ppm, a double letter labelling scheme is shown to indicate that these peaks can be equally assigned to any of two diastereotopic hydrogens.

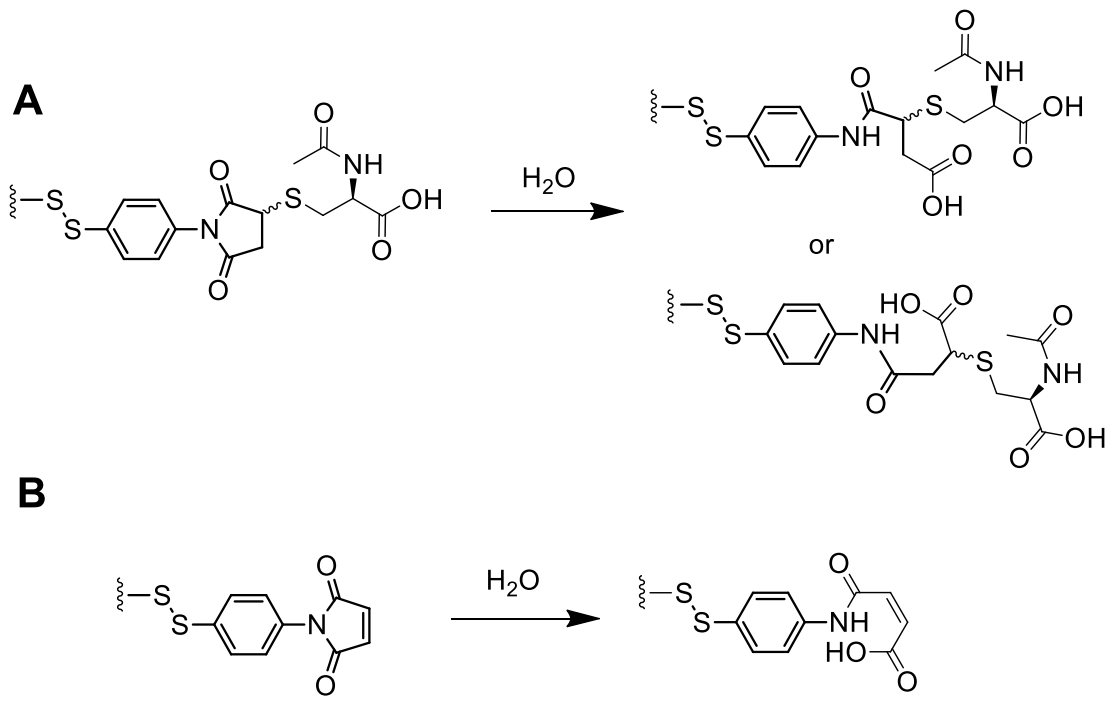

Scheme 1S. A. Products of the hydrolysis of the succinimide moiety of **2** and **3**. B. Product of hydrolysis of the maleimide moiety of **3**.

Hydrolysis of 2 and 3. The kinetic of hydrolysis of **2** and **3** in solution was quantified following changes in the UV/Vis absorbance. The increase in absorbance at 300 nm of a solution of **2** follows a 1st order kinetic, with a rate constant that is proportional to the concentration of the OH^- specie, consistent with the base-catalysed hydrolysis of the succinimide moiety (Figure 4S A, B, C and G).[39,41] For **3**, the absorbance follows a bi-exponential increase, consistent with the hydrolysis of the succinimide (slow hydrolysis) and maleimide (fast hydrolysis) moieties (Figure 4S D, E and F). As with **2**, the rate constants are proportional to the concentration of OH^-, consistent with base-catalysed hydrolysis of the imide moieties (Figure 4S G). The slow process is assigned to the hydrolysis of the succinimide moiety by comparison with the hydrolysis of **2**. The observed faster hydrolysis of the maleimide moiety in relation to the succinimide is consistent with literature data.[38,39]

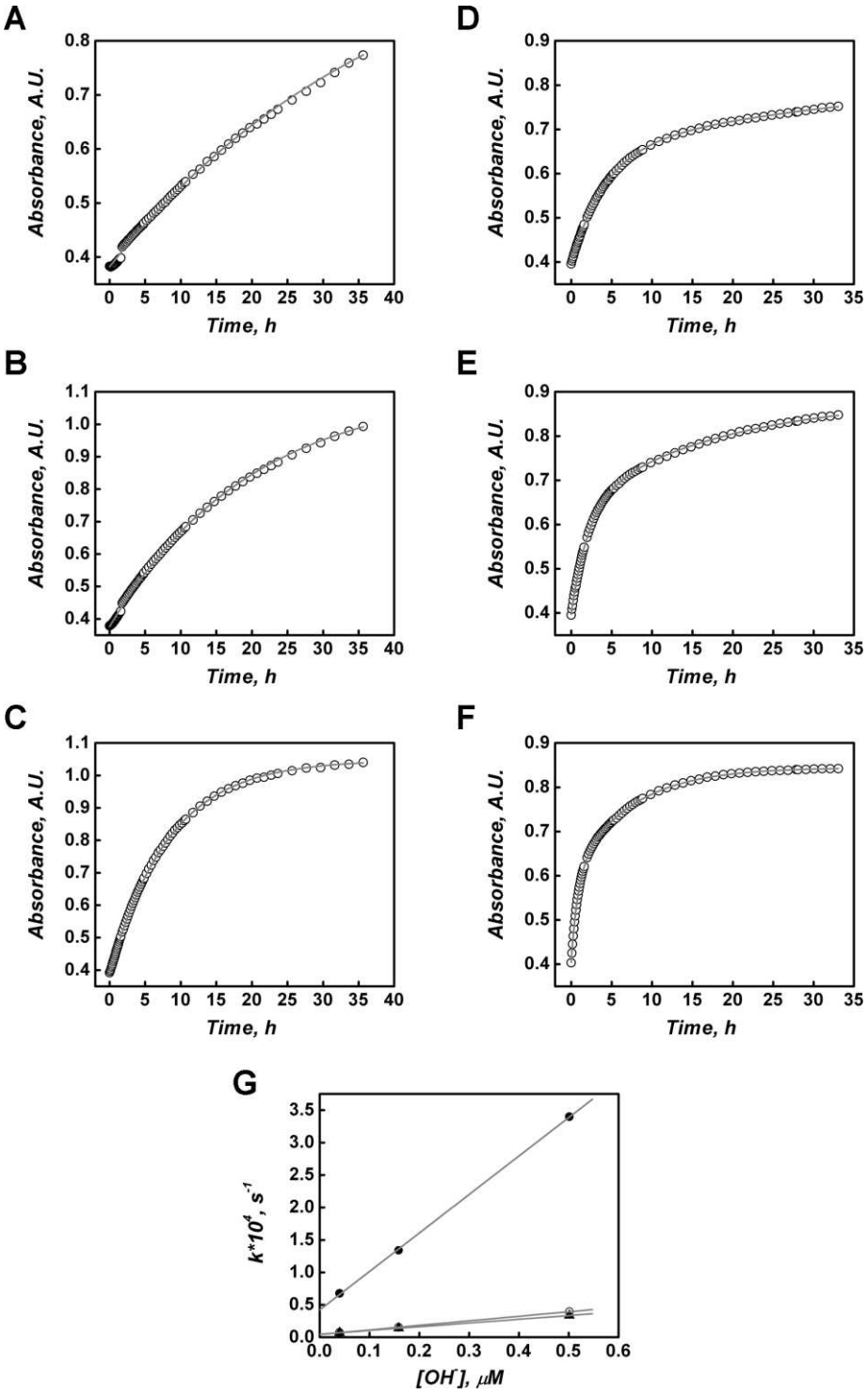

Figure 4S. Variation of the absorbance at 300 nm of a solution of **2** (120 μM) in phosphate buffer (80 mM) at pH 6.6 (A), 7.2 (B) and 7.7 (C) (empty circles) and fitting to a first order kinetic process, using the program Specfit 3.0 (grey line). Variation of the absorbance at 300 nm of a solution of **3** (41 μM) in phosphate buffer (80 mM) at pH 6.6 (D), 7.2 (E) and 7.7 (F) (empty circles) and fitting to a bi-exponential kinetic process, using the program Specfit 3.0 (grey line).[48] Panel G shows the correlation ($R^2 > 0.999$ in

all cases) between the calculated rate constants *k* and the concentration of OH^- . The rate constant for the hydrolysis of the succinimide moieties of 2 is represented by filled triangles, for the hydrolysis of the same moiety in **3** by empty circles and for the hydrolysis of the maleimide moiety of **3** by filled circles. See Table 1 for the numerical values of *k*...

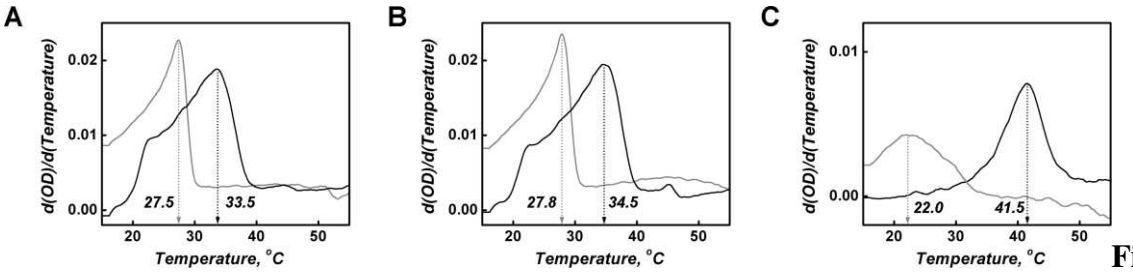

Figure 5S. A. Graphical representation of the first derivative of the gel melting curves for hydrogel **2** (see Figure 3), showing the melting temperature (Tm) as the absolute maximum of the curve (i.e., the inflexion point on the original curve shown in Figure 3).The black trace corresponds to the heating phase of the cycle and the grey trace to the cooling phase of the cycle. B. Idem for hydrogel **2** after reduction with DTT and oxidation with H_2O_2. C. Idem for hydrogel **3**.

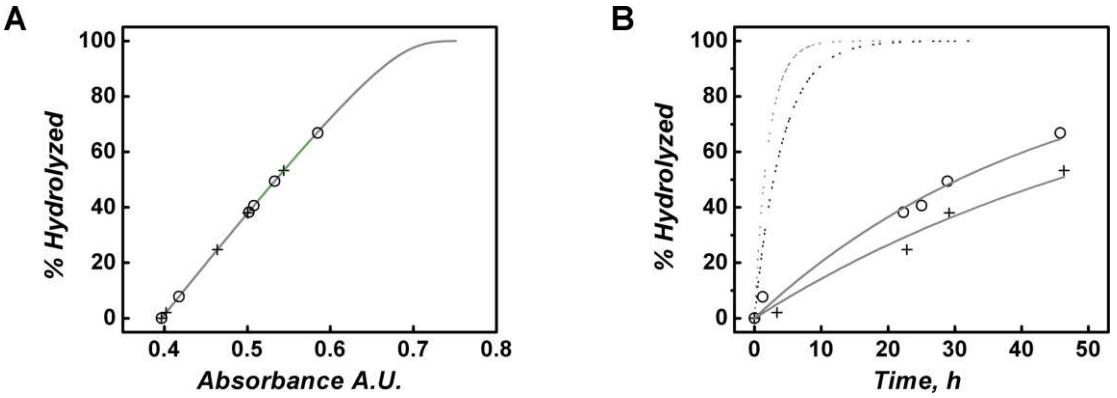

Figure 6S. A. Grey line: correlation between the percentage of hydrolyzed **3** with either or both maleimide and succinimide hydrolyzed and the increase in absorbance at 300 nm calculated from the

fitting of the UV/Vis data of 3 (41 μM) with Specfit 3.0 (see Figure 4S and Table 1).[48] Empty dots: absorbance of samples of **3** obtained by diluting gel **3** (15 mM kept at pH 7.2) down to 41 μM. The dots have been graphically placed over the grey line in order to estimate the percentage of hydrolysed **3** in the hydrogel form at different time intervals. Crosses: idem for gel **3** kept at pH 6.6. B. Percentage of hydrolysed **3** hydrogel (15 mM) in 80 mM phosphate buffer pH 7.2 (○) and pH 6.6 (**+**) with time as determined graphically in A and fit to a first order kinetic process (solid grey line). See Table 1 for rate constants. For comparison, the increase in hydrolysed **3** in solution, calculated from the fitting of the hydrolysis data (see Figure 4 and Table 1), is also shown as dashed lines (grey: pH 7.2; black: pH 6.6).

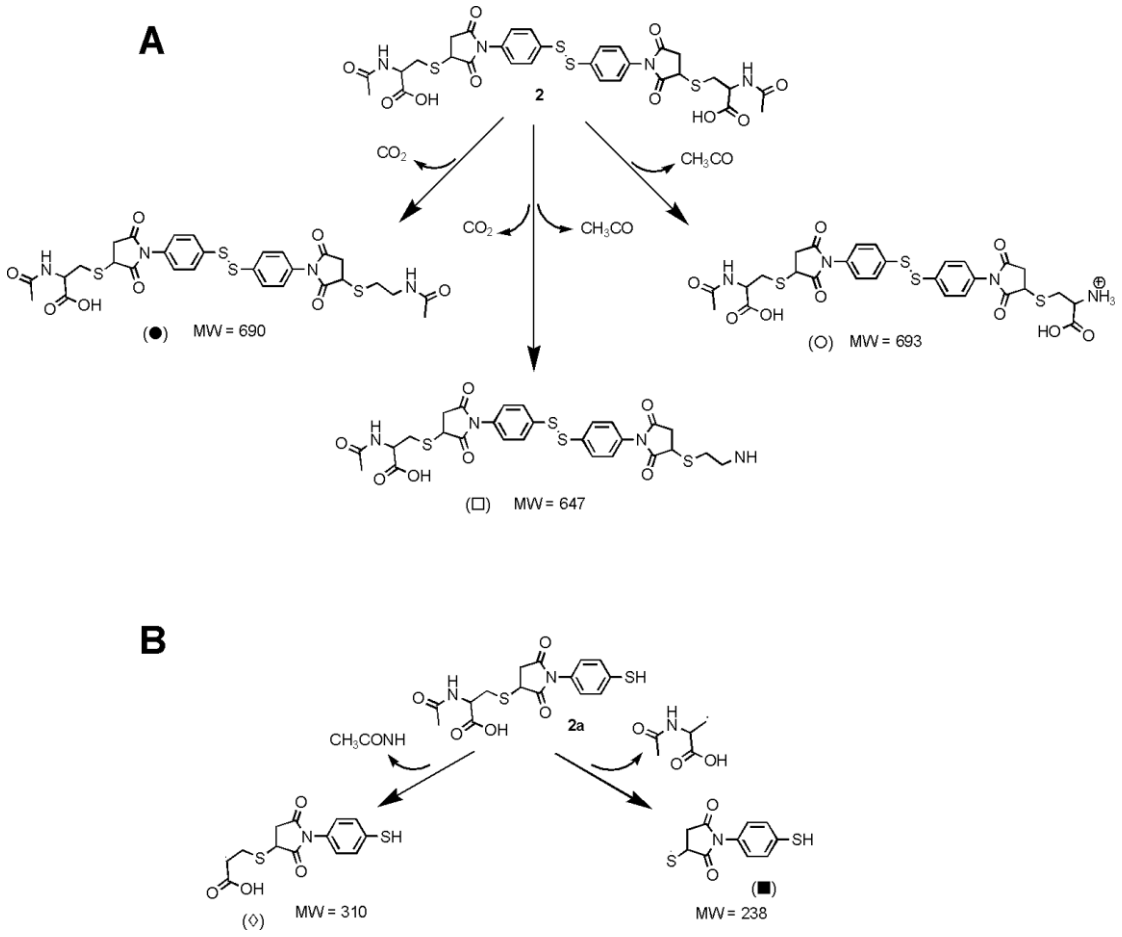

Scheme 2S. Fragments of **2** (A) and **2a** (B) detected in the LC-MS of samples of hydrogel **2** treated with DTT and H_2O_2. (see Figure 4).

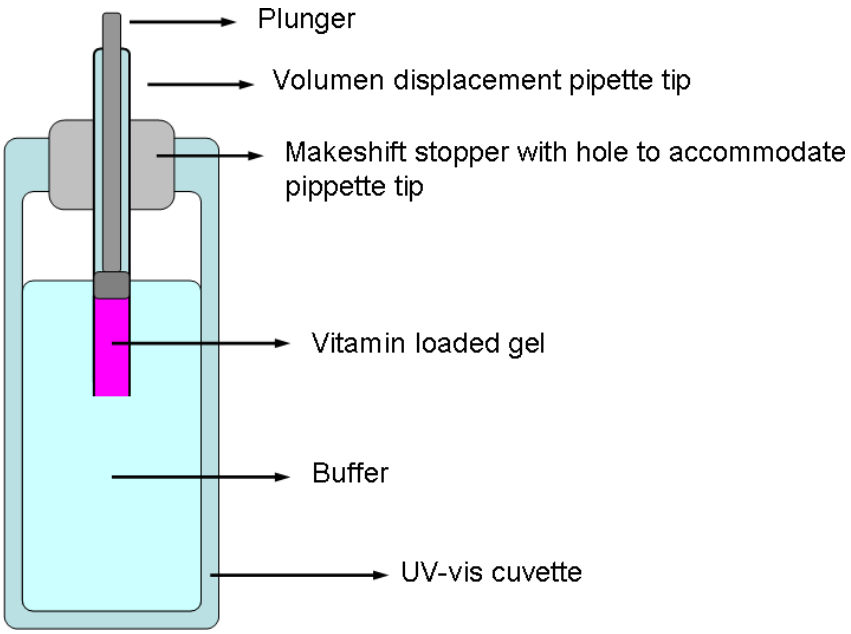

Figure 7S. Schematic representation of the UV/Vis cell adapted for the vitamin release experiments.

Entry for the Table of Contents (Please choose one layout only)

Layout 1:

Catch Phrase

*Author(s), Corresponding Author(s)** …….…… Page – Page

((The TOC Graphic should not exceed the size of this area))

Text for Table of Contents, max. 450 characters.

Layout 2:

Multiresponsive LMWH

Lilia Milanesi, Christopher Hunter, Nadejda Tzokova, Jonathan P. Waltho and Salvador Tomas** …….…… Page – Page

Versatile low molecular weight hydrogelators: achieving multiresponsivenes via a modular design

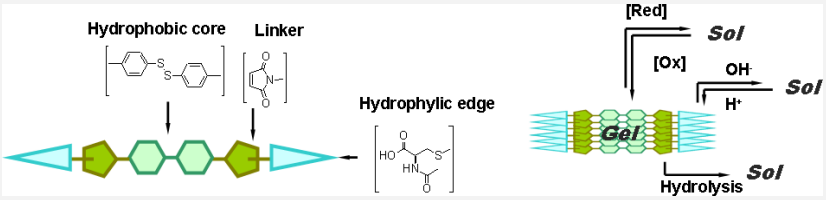

Our limited ability in predicting self-assembly in water hampers the design of new hydrogelators. The problem is exacerbated when multiresponivenes is required: the need of introducing multiple chemical switches imposes further limitations on design. Here we present effcient multiresponsive hydrogelators based on a modular design. Each module bears a chemical switch with the appropiate hydrophiliciy to make it compatible with gel assembly.